Ostwald ripening of rod-shaped α-Fe particles in a Cu matrix

Ostwald ripening of rod-shaped α-Fe particles in a Cu matrix

R. Monzen[a,*], T. Tada[a], T. Seo[a], K. Higashimine[b]

[a]Department of Mechanical Systems Engineering, Kanazawa University, 2-40-20 Kodatsuno, Kanazawa, Ishikawa 920-8667, Japan

[b]Center for Nano Materials and Technology, Japan Advanced Institute of Science and Technology, 1-1 Asahidai, Tatsunokuchi, Ishikawa 923-1292, Japan

Abstract

The coarsening behavior of rod-shaped α-Fe particles in Cu–1.3 wt% Fe and Cu–1.3 wt% Fe–1.2 wt% Sb alloys during aging at 700 °C has been studied by transmission electron microscopy and electric resistivity. The kinetics of the decay of supersaturation with aging time t for both alloys are coincident with the $t^{-1/3}$ law. The coarsening kinetics of the cylindrical radius of the Fe particles obey the $t^{1/3}$ law. Using the Lifshitz-Slyozov-Wagner theory modified for the case of rod-shaped particles by Speich and Oriani, the maximum value of the Cu/α-Fe interfacial energy γ and the volume diffusivity D of Fe in Cu for the Cu–Fe alloy are independently derived to be 1.2 J/m^2 and 3.7×10^{-18} m^2/s. Adding Sb to the Cu–Fe alloy decreases the values of γ and D.

keywords: Copper-iron; Rod-shaped α-iron particles; Interfacial energy; Diffusion coefficient; Coarsening kinetics; Antimony addition

1. Introduction

Aging of a solution-treated Cu–Fe alloy first produces coherent γ-Fe precipitate particles in a Cu matrix [1]. The γ-Fe particles transform martensitically to α-Fe by plastic deformation of the alloy [2-5]. The α-Fe particles satisfy the Kurdjumov–Sachs (K–S) orientation relationship to the matrix; $\{111\}_{Cu}//\{110\}_{Fe}$ and $<110>_{Cu}//<111>_{Fe}$. Particular martensite variants are formed preferentially by an uniaxial tensile deformtion [3-5].

Fujii *et al.* [6] have studied the morphological changes and growth kinetics of the transformed α-Fe particles in Cu single crystals by transmission electron microscopy (TEM). The α-Fe particles were elongated along $<110>_{Cu}$ ($//<111>_{Fe}$) according to the K–S orientation relationship. Using the Lifshitz-Slyozov-Wagner (LSW) [7,8] theory of Ostwald ripening, the interfacial energy between Cu and α-Fe was estimated to be approximately 3.3 J/m^2. On the other hand, Monzen and Kita [9] have investigated the coarsening of α-Fe particles with no specific orientation relationship to the Cu matrix, produced by recrystallization on annealing of aged and deformed polycrystals of Cu–Fe alloys. The shape of the α-Fe particles was consistently nearly spherical during aging. TEM was used to measure the average size of the α-Fe particles, and electrical resistivity (ER) to measure the concentration of Fe in solid solution in equilibrium with Fe particles of various sizes. The coarsening behavior of the spherical α-Fe particles was consistent with the prediction of the LSW theory. From the data on coarsening alone, independent values of the diffusion coefficient of Fe in the Cu matrix and the Cu/α-Fe interfacial energy were evaluated. The interfacial energy was 0.52 J/m^2 much smaller than the value of 3.3 J/m^2 determined by Fujii *et al*. [6]. The effect of Sb on the coarsening of the spherical α-Fe particles in a Cu–Fe alloy has also been examined by both TEM and ER [10]. It was found that the Sb addition decreased both the volume diffusivity of Fe in Cu and the Cu/α-Fe interfacial energy by segregation of Sb at the incoherent interfaces.

Speich and Oriani [11] have examined the rates of coarsening of rod-shaped Cu particles

in an Fe–Cu alloy by TEM. The average cylindrical radius of rod-shaped particles increased with aging time t as $t^{1/3}$, as deduced by the LSW theory. Moreover, a LSW equation, modified for both the nonsphericity of the diffusion field and the refoemulation of the Gibbs-Thomson equation for the case of nonspherical particles, was derived.

The purpose of the present study is to investigate the coarsening kinetics of the rod-shaped α-Fe particles in Cu–1.3 wt% Fe and Cu–1.3 wt% Fe–1.2 wt% Sb alloys. Using the LSW equation modified for rod-shaped particles by Speich and Oriani, the Cu/α-Fe interfacial energy and the diffusion coefficient of Fe in Cu are independently derived from measurements of the particle size by TEM and the Fe concentration in the Cu matrix by ER.

2. Experimental procedures

Single crystals of a Cu–1.3 wt% Fe alloy were grown by the Bridgman method with a seed. Tensile specimens with a dimension of 3×5×40 mm^3 were cut from the single crystals. These specimens had approximately the identical tensile axis, parallel to $[419]_{Cu}$. About half of the specimens were Sb-doped at 950 °C for 96 h in an Ar atmosphere with a powder pack method. A mixture of Cu (10 parts), Al_2O_3 (10 parts) and Sb (1part) powders was used for this purpose. A chemical analysis showed that the Sb-doped specimens contained 1.2 wt% Sb. All specimens were solution-treated at 980 °C for 3 h, quenched into water and aged at 700 °C for 8 h to precipitate γ-Fe particles. Then they were strained at −196 °C by 25 % to introduce a γ to α martensitic transformation. The 25 % straining led to the transformation in nearly all the Fe particles in Sb-free and Sb-doped specimens. After the strained specimens were aged at 700 °C for times up to 96 h, ER measurements were made by a constant electrical current method. For the Cu–1.3 wt% Fe–1.2 wt% Sb alloy, the Fe concentrations in the Cu matrix were determined by applying the experimental data obtained by Linde [12], after the resisitivity increment caused by 1.2 wt% Sb in the matrix was removed using the data in the literature [13], as in our previous study [10].

The strained specimens also were sliced parallel to the primary slip plane $[\bar{1}1\bar{1}]_{Cu}$ to form discs. TEM specimens were prepared from the discs by electropolishing using a phosphoric acid solution. Microscopy was carried out with a HITACHI H-9000NAR microscope operating at 300 kV.

3. Results and discussion

3.1. Kinetics of particle growth and depletion of supersaturation

Specimens aged at 700 °C after straining at −196 °C were observed using the incident electron beam parallel to $[\bar{1}1\bar{1}]_{Cu}$. As shown in Fig. 1, most α-Fe particles elongated along $[110]_{Cu}$ as the particles became larger. Analyses of selected-area diffraction patterns taken from several regions containing the particles elongated along $[110]_{Cu}$ revealed that the α-Fe particles satisfied nearly the K–S orientation relationship,

$$(\bar{1}1\bar{1})_{Cu} // (110)_{Fe}, \qquad [110]_{Cu} // [\bar{1}1\bar{1}]_{Fe}$$

and

$$(\bar{1}1\bar{1})_{Cu} // (110)_{Fe}, \qquad [110]_{Cu} // [\bar{1}1\bar{1}]_{Fe}$$

to the Cu matrix, in agreement with previous studies [3-5]. The mean aspect ratio β ($=l/2r$) of the major axis (l) to the minor axis ($2r$) of the Fe particles is plotted against aging time t for Cu–Fe and Cu–Fe–Sb alloys in Fig. 2. For both alloys, β increases with increasing t and becomes a constant value of about 3 beyond about 24 h.

The LSW treatment is restricted to the case of spherical particles. Speich and Oriani [11] have extended the LSW theory to the case of nonspherical particles. The equilibrium shape of the particles is that of rods with hemispherical caps, and is due to the anisotropy in the interfacial energy. They have shown that the coarsening kinetics of the rod-shaped particles are of the form

$$\bar{r}^3 - \bar{r}_0^3 = Kt\,, \qquad (1)$$

where

$$K=8\gamma DC_e V_m^2/9RT\beta\ln(2\beta). \quad (2)$$

Here, $\bar{r}$ is the mean cylindrical radius of the rod-shaped particles, $\bar{r}_0$ is the integration constant, D is the volume diffusivity of solute in the bulk, γ is the interfacial energy at the centers of the end caps of the rod-shaped particles, C_e is the solubility of solute in the bulk, V_m is the molar volume of the particles and RT has its usual meaning. In the present study, V_m is caluculated to be 7.11×10^{-6} m^3/mol and $\bar{r}_0$ is taken as the average radius (22 or 16 nm) of the α-Fe martensite particles after deformation at −196 °C. It may be noted that the value of V_m is almost identical to the value of 7.09×10^{-6} m^3/mol for Cu. On the other hand, according to the LSW theory, the rate constant K is expressed as

$$K=8\gamma DC_e V_m^2/9RT. \quad (3)$$

Following Eq. (1), plots of $(\bar{r}^3-\bar{r}_0^3)$ vs. t are given in Fig. 3. For each experimental point, about 200 particles were measured. Excepting the initial stage of aging, a linear relationship is found between $(\bar{r}^3-\bar{r}_0^3)$ and t. It is also evident that the Sb addition to the Cu–Fe alloy decreases the growth rate of the particles, similar to the result for the spherical α-Fe particles in our previous study [10]. Since the aspect ratio became a constant value of 3 after aging for 24 h, the straight lines in Fig. 3 were drawn by the least-squares method using experimental points above 24 h. Table 1 lists the values of the rate constant K obtained from their slopes.

The distributions of the cylindrical radius of the rod-shaped Fe particles were almost independent of t and were similar to those for the spherical Fe particles in our previous studies [9, 10, 14].

The LSW theory of coarsening modified by Ardell [15] predicts that, for the coarsening of the rod-shaped particles, the concentration of solute in the matrix after coarsening time t is written as

$$C-C_e=(kt)^{-1/3}, \quad (4)$$

where

$$k=D(RT/\gamma C_e)^2/9\beta\ln(2\beta). \quad (5)$$

Figure 4 shows the variation in the Fe concentration C as a function of $t^{-1/3}$ for Cu–Fe and Cu–Fe–Sb alloys. C rapidly decreases at the initial stage of aging and over about 24 h the date display a linearity. This corresponds well to the result in Fig. 2. That is, the true Ostwald ripening of rod-shaped Fe particles begins after the aspect ratio becomes constant. The slopes of the straight lines yield values of $k^{-1/3}$. Table 1 lists these values, together with the equilibrium concentrations C_e of Fe in the Cu matrix, obtained from the intercepts at $t^{-1/3}=0$. The values of C_e are nearly the same and agree with the value of about 460 mol/m^3 at 700 °C for spherical α-Fe particles in Cu–Fe and Cu–Fe–Sb alloys [9, 10].

3.2. Diffusivity and interfacial energy

Eq. (2), derived by Speich and Oriani [11], is valid only when the aspect ratio is very large. In their derivation, the flux to the lateral (side) surface of a rod was taken into account, but the flux to the two edge (circular) surface was not. Thus, Eq. (2) should be used with a caution for a case with the aspect ratio of the order of 3. Nevertheless, we will try estimating independently the interfacial energy γ and diffusivity D using Eqs. (2) and (5).

From Eqs. (2) and (5), γ and D are given as

(6)

and

. (7)

Table 1 tabulates the values of γ and D calculated using these equations. Here, $\beta=3$ was used.

The existence of Sb in the Cu matrix causes a reduction in D, in agreement with the previous study [10]. The D value for the Cu–Fe alloy is nearly identical to the value of 3.7×10^{-16} m^2/s reporeted in the literature [16]. The D values for the Cu–Fe and Cu–Fe–Sb alloys also are very similar to the values of 3.5×10^{-16} [9] and 2.0×10^{-16} m^2/s [10] for the spherical α-Fe particles in the same alloys, previously obtained using the LSW theory. This

indicates that the use of Eq. (2) would be valid even in the case with the aspect ratio equal to only 3 in the present study. On the other hand, the value of γ for the rod-shaped particles in the Cu–Fe alloy is 1.2 J/m^2 larger than the value of 0.52 J/m^2 for the spherical α-Fe particles in Cu–Fe alloys [9]. Moreover, the addition of Sb to the Cu–Fe alloy reduces the γ value. This resembles the result of the previous study and is caused by segregation of Sb at the Cu/α-Fe interfaces [10].

The elongated shape of the α-Fe particles is understood to be based on the large anisotropy in the Cu/α-Fe interfacial energy. That is, an Fe particle may take a rodlike shape with which the total interfacial energy becomes smaller than that achieved when it would take a spherical shape with the identical volume. If this is the case, the minimum energy of the interface encircling the rod-shaped Fe particles should be smaller than the interfacial energy γ_s for the spherical Fe particles. According to Speich and Oriani [11], $\gamma/\gamma_a=\beta$, where γ_a is the energy of the interface normal to the short axis of a rod-shaped particle. γ and γ_a are the maximum and minimum values of interfacial energy respectively. In the present case, γ_a (0.39 J/m^2) < γ_s (0.52 J/m^2 [9]) < γ (1.2 J/m^2). Therefore, the experimentally determined value of 1.2 J/m^2 may be reasonably accepted as the maximum value of the interfacial energy.

Fujii *et al.* [6] have examined the growth kinetics of the α-Fe martensite particles in single crystals of a Cu–Fe alloy. Although the α-Fe particles grew into elongated ellipsoids along <110>$_{Cu}$, using the LSW theory, the Cu/α-Fe interfacial energy was estimated to be approximately 3.3 J/m^2, which is much larger than the value of 1.2 J/m^2 obtained in the present study. Therefore we attempted to determine the interfacial energy using the LSW theory by the same method as by Fujii *et al*. The shape of the Fe particles was assumed to be a spheroid described in the x-y-z coordinates by $x^2/(l/2)^2+(y^2+z^2)/r^2\leq 1$. Further, the radius of a sphere of volume equal to that of the assumed spheroid was calculated. Figure 5 shows the data for the Cu–Fe alloy, plotted in the form $(\bar{r}^3-\bar{r}_0^3)$ vs. *t*. A linearity is absent between $(\bar{r}^3-\bar{r}_0^3)$ and *t* during aging up to about 24 h. That is, the growth rate of the α-Fe particles is not constant with aging owing to the change in the aspect ratio with *t*, similar to the

observation by Fujii *et al*. However, the linearlity is seen over about 24 h. In order to obtain a rough value of the interfacial energy γ at the early stage of aging, the $(\overline{r}^3 - \overline{r}_0^3)$–$t$ curve was approximated by a dotted line drawn with the least-squares method, as shown in Fig. 5.

From Eq. (3) using K=3.19×10^{-28} m^3/s? and values of C_e and D in Table 1, γ was estimated as 3.1 J/m^2. This value agrees with the value of 3.3 J/m^2 obtained by Fujii *et al*. [6]. On the other hand, the straight line (K=6.40×10^{-29} m^3/s?) at the later stage of aging in Fig. 5 yields a value of 0.62 J/m^2. Interestingly, this value is close to 0.52 J/m^2 for the spherical Fe particles [9].

4. Conclusions

(1) The average cylindrical radius of rod-shaped α-Fe particles in Cu–1.3 wt% Fe and Cu–1.3 wt% Fe–1.2 wt% Sb alloys aged at 700 °C increases with aging time t as $t^{1/3}$, as predicted by the LSW theory. The kinetics of the depletion of supersaturation with t are in agreement with the predicted $t^{-1/3}$ time law.

(2) Application of the LSW theory modified for rod-shaped particles by Speich and Oriani [11] has enabled independent calculation of the maximum value of the Cu/α-Fe interfacial energy γ and the diffusivity D of Fe in Cu during coarsening. The values of γ and D for the Cu–Fe alloy are estimated as 1.2 J/m^2 and 3.7×10^{-18} m^2/s respectively. The D value agrees with literature diffusion data. Sb added to the Cu–Fe alloy reduces the values of γ and D.

Acknowlegement

We thank Professor K. Tazaki, Kanazawa University, for the provision of laboratory facilities.

References

[1] K. E. Easterling, H. M. Miekk-Oja, Acta Metall. 15 (1967) 1133.

[2] K. R. Kinsman, J. W. Sprys, R. J. Asar, Acta Metall. 23 (1975) 1431.

[3] M. Kato, R. Monzen, T. Mori, Acta Metall. 26 (1978) 605.

[4] R. Monzen, A. Sato, T. Mori, Trans. Japan Inst. Metals 22 (1981) 65.

[5] M. Kato, T. Fujii, Y. Hoshino, T. Mori, J. Japan Inst. Metals 56 (1992) 865.

[6] T. Fujii, M. Kato, A. Sato, Mater. Trans. Japan Inst. Metals 32 (1991) 229 .

[7] I. M. Lifshitz, V. V. Slyozov, J. Phys. Chem. Solids 19 (1961) 35.

[8] C. Wagner, Z. Elektrochem. 65 (1961) 581.

[9] R. Monzen, K. Kita, Phil. Mag. Lett. 82 (2002) 373.

[10] R. Monzen, T. Tada, K. Kita, Phil. Mag. Lett. 83 (2003) 433.

[11] G. R. Speich, R. A. Oriani, Trans. Metall. Soc. AIME 233 (1965) 623.

[12] J. O. Linde, Ann. D. Phy. 15 (1932) 219 .

[13] F. Pawlek, K. Reichel, Z. Metallk. 47 (1956) 347.

[14] K. Kita, R. Monzen, Scripta Metall. 43 (2000) 1039.

[15] A. J. Ardell, Acta Metall. 16 (1968) 511.

[16] Japan Inst. Metals, Kinzoku Data Book, Maruzen Press, Tokyo, 1993, p. 21.

Figure captions

Fig. 1. Transmission electron microscope of rod-shaped α-Fe particles in a Cu–1wt% Fe alloy aged at 700 °C for 96 h. The incident electron beam direction is parallel to $[\bar{1}1\bar{1}]_{Cu}$.

Fig. 2. Change in the mean aspect ration β of rod-shaped Fe particles in alloys containing 1.3 wt% Fe and 1.3 wt% Fe–1.2 wt% Sb aged at 700 °C with aging time t.

Fig. 3. Coarsening plot of the cylindrical radius of rod-shaped Fe particles in alloys containing 1.3 wt% Fe and 1.3 wt% Fe–1.2 wt% Sb aged at 700 °C.

Fig. 4. Change in the Fe concentration C in the matrix of Cu–Fe and Cu–Fe–Sb alloys aged at 700 °C with $t^{-1/3}$.

Fig. 5. Coarsening plot of the equivalent spherical radius of rod-shaped particles in a Cu–Fe alloy aged at 700 °C.

Table 1. Values of K, $k^{-1/3}$, C_e, D and γ for rod-shaped α-Fe particles in Cu–1.3 wt% Fe and Cu–1.3 wt% Fe–1.2 wt% Sb alloys.

Table 1. Values of K, $k^{-1/3}$, C_e, D and γ for rod-shaped α-Fe particles in Cu–1.0 wt% Fe and Cu–1.0 wt% Fe–1.2 wt% Sb alloys.

Specimen	K (10^{-28} m^3/s)	$k^{-1/3}$(mol s$^{1/3}$/m^3)	C_e (mol/m^3)	D (10^{-16} m^2/ s)	γ (J/m^2)
1.0 Fe	2.55±0.58	1650±420	460	3.9	1.3
1.0 Fe–1.2 Sb	1.20±0.52	1620±450	450	2.5	1.0

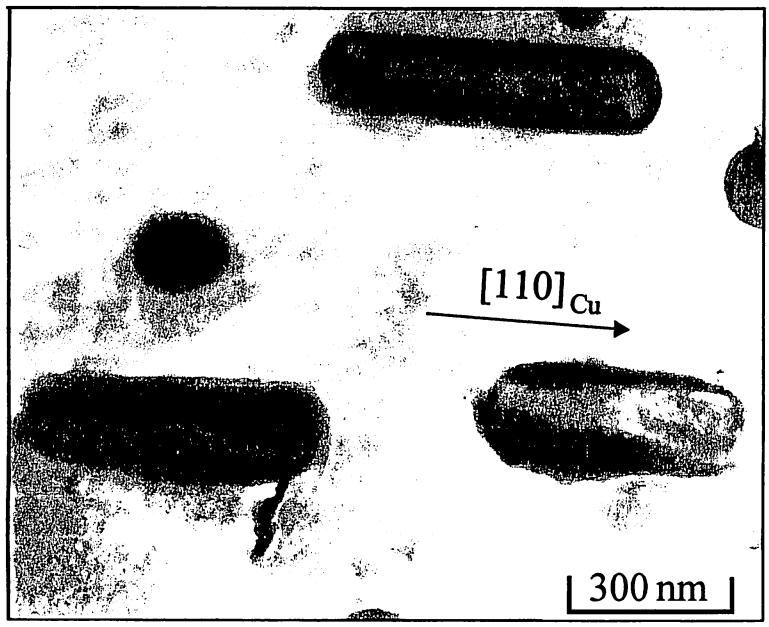

Fig. 1. Transmission electron ~~microscopy~~ micrograph of rod-shaped α-Fe particles in a Cu–1.0 wt% Fe alloy aged at 700 °C for 96 h. The incident electron beam direction is parallel to $[\bar{1}1\bar{1}]_{Cu}$.

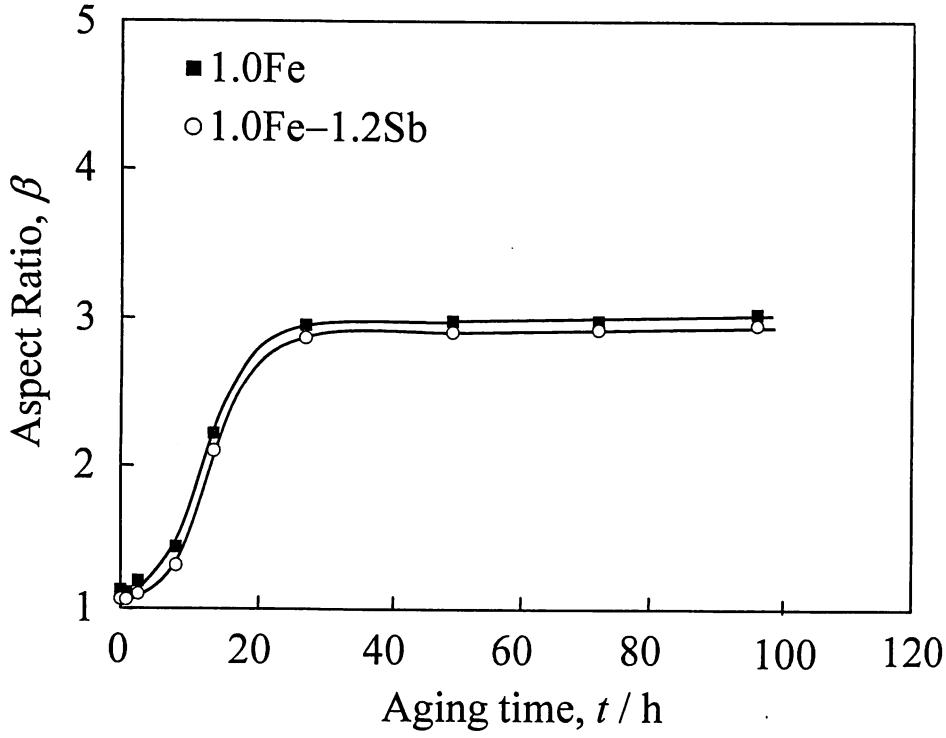

Fig. 2. Change in the mean aspect ratio β of rod-shaped Fe particles in alloys containing 1.0 wt% Fe and 1.0 wt% Fe–1.2 wt% Sb aged at 700 °C with aging time t.

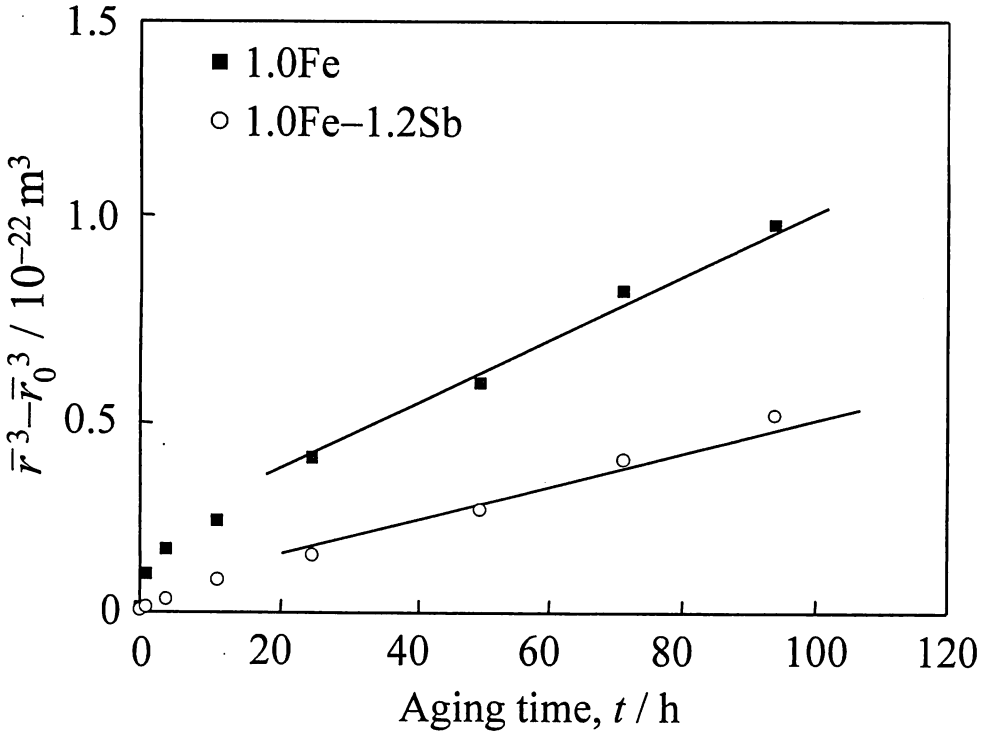

Fig. 3. Coarsening plots of the cylindrical radius of rod-shaped Fe particles in alloys containing 1.0wt% Fe and 1.0wt% Fe–1.2 wt% Sb aged at 700 °C .

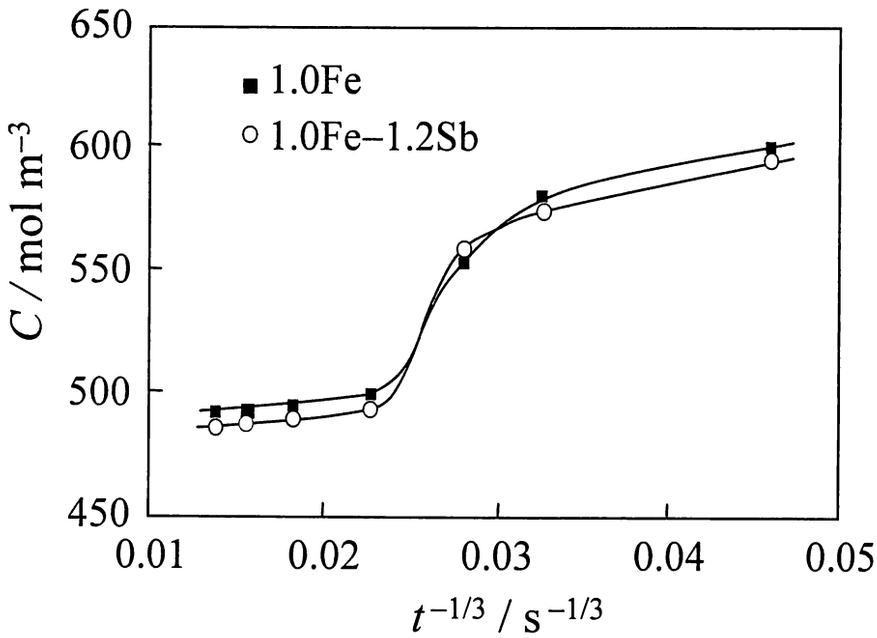

Fig. 4. Change in the Fe concentration C in the matrix of Cu–Fe and Cu–Fe–Sb alloys aged at 700 °C with $t^{-1/3}$.

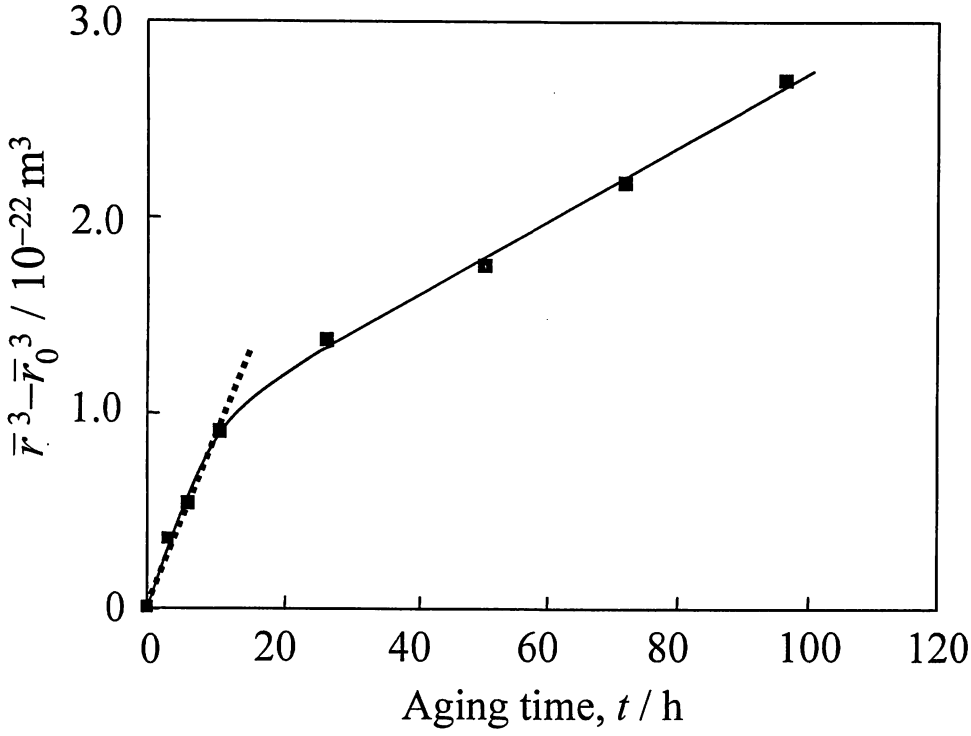

Fig. 5. Coarsening plot of the equivalent spherical radius $\overline{r}$ of rod-shaped particles in a Cu–Fe alloy aged at 700 °C.